

To Self-Organized Criticality and Avalanches

Lecture by: P. H. Diamond, Note by: Jung-Tsung Li

Lecture dates: May 28 and 30, 2019

1 A brief intellectual history of SOC

So far we have covered diffusion and percolation, the phase transition, intermittency and Levy distribution. There was story emerged from hydrology which address the question of charactering time scales and time series, and eventually the story lead to Hurst (H) parameter and the relation to Holder exponent. On the other hand, we also learn that intermittency gains multiplicative processes and log-normality. Separate from that but related is the Pareto-Levy distribution. Pareto was interested in concentrated distribution of the wealth in the society. Levy was interested in generalizing central limited theorem – identify the broader class of fixed points in function space and discover the levy walk.

See Fig. 1 for the flowchart of the storyline. Long story short, the hydrology line is interested in time series and turbulence. The intermittency line is interested in random walk and intermittency in dynamical systems. The two story lines were eventually united by the ideas of fractals and the fractal model introduced by Mandelbrot and Wallis [1]. They realized that the fractal model unifies the intermittency and turbulence with the concept of the strange behavior in time series. A deeper meaning of it is the connection between spatial and temporal self-similar structures.

Note that the $H \rightarrow 1$ is ubiquitous phenomena of the $1/f$ “noise”. (It’s not really the noise but instead a $1/f$ distribution/fluctuation). The $H \rightarrow 1$ has ballistic propagation, $\delta l \sim t$, which suggests a self-similarity. This idea lead people to wonder if there was a simple physical model that manifests $1/f$ noise. The story eventually leads to the development of self-organized criticality (SOC) in the 80’s [2, 3].

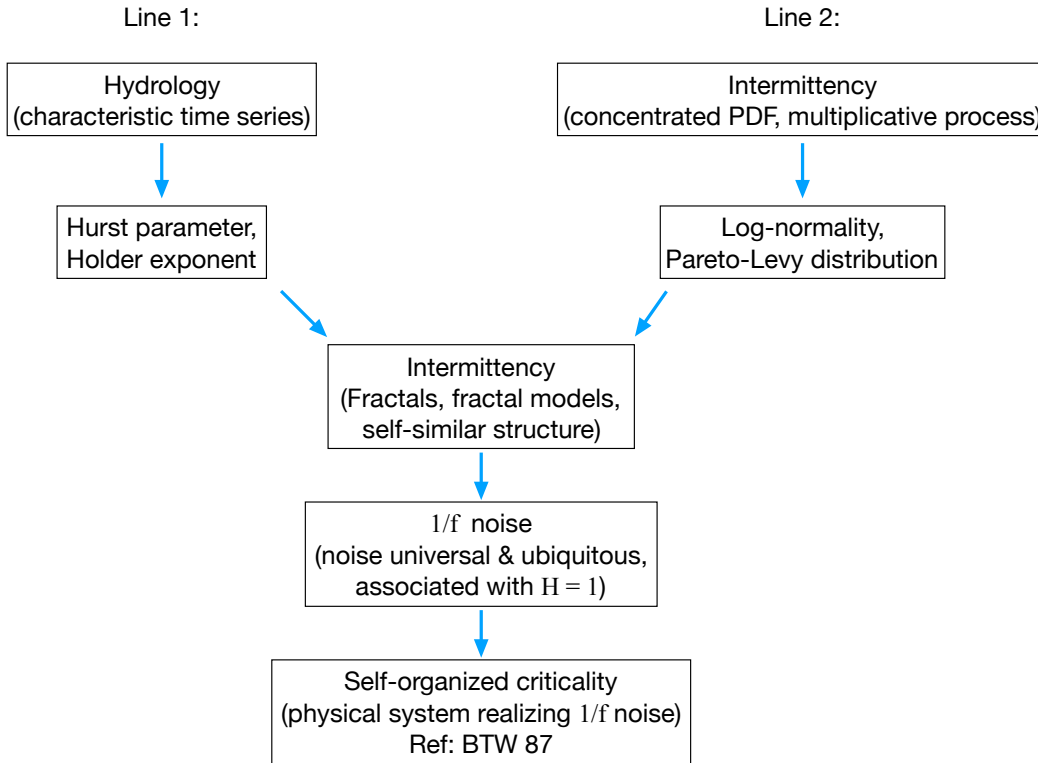


Figure 1: A brief history of the self-organized criticality.

2 Log-normal distribution, $1/f$ distribution and $1/f$ noise

Two critical factors in SOC are Zipf's law and $1/f$ noise. They are related but *different*.

- **Zipf's law** [4]: the probability of the event at x is $P(x) \sim 1/x$ – big event is rare and small event is frequent. In Sec. 2.1, we will show that Zipf's law is a good fit to log-normal distribution for a broad range and is natural for the multiplicative processes.
- **$1/f$ noise**: the frequency spectrum is $\langle(\Delta B)^2\rangle_\omega \sim 1/\omega$. In section 2.2, we will show how to get $1/f$ noise from $1/f$ distribution.

Both suggest a self-similar structure, which indicates the absence of a clear scale and the rarity of large events. $1/f$ is related to $H \rightarrow 1$, which is persistent.

2.1 Zipf's fit to log-normal distribution and $1/f$ distribution

Below we will follow Montroll & Shlesinger 1982 [5] to show that Zipf's law is a good fit to a log-normal to a wide range. An $1/f$ distribution function diverges in the full range $0 < f < \infty$ since its normalization diverges as $\log f$ when $f \rightarrow 0$ and $f \rightarrow \infty$. As a result,

a purely $1/f$ distribution is not normalizable. On the other hand, a distribution with large dispersion can be mimicked by a $1/x$ distribution over a wide range of x . So to get an overall normalizable distribution and a $1/f$ -like behavior in the intermediate range, one shall use log-normal distribution of the variable $\log x$ [5]:

$$F(\log x) = \frac{\exp\left[-(\log x - \log \bar{x})^2 / 2\sigma^2\right]}{\sqrt{2\pi\sigma^2}}, \quad (1)$$

where \bar{x} and σ stand for the mean and dispersion of the distribution, respectively. The probability that x/\bar{x} lies in $d(x/\bar{x})$ at x/\bar{x} is given by

$$\begin{aligned} P\left(\frac{x}{\bar{x}}\right) &= g\left(\frac{x}{\bar{x}}\right) d\left(\frac{x}{\bar{x}}\right) \\ &= \frac{\exp\left[-\log^2(x/\bar{x}) / 2\sigma^2\right]}{\sqrt{2\pi\sigma^2}} \frac{1}{(x/\bar{x})} d\left(\frac{x}{\bar{x}}\right), \end{aligned} \quad (2)$$

where $g(x/\bar{x})$ is the log-normal probability distribution function (PDF). Letting $x \equiv f\bar{x}$ and taking $\log g$ as a function of f , we obtain

$$\begin{aligned} \log g(f) &= \frac{-(\log f)^2}{2\sigma^2} - \frac{1}{2} \log(2\pi\sigma^2) - \log f \\ &= -\log f + \text{variance corrections.} \end{aligned} \quad (3)$$

Equation (3) indicates that, for a large value of σ , the distribution function $g(f)$ would become more close to a $1/f$ distribution. This is achieved when the system has a large number of multiplicative events. In the multiplicative processes, the square of the total dispersion is scaled as the total number of event, N ,

$$\sigma^2 \equiv \sum_{j=1}^N \sigma_j^2 = N\bar{\sigma}^2, \quad (4)$$

so the larger N value, the greater the number of decades that the distribution function $g(f)$ mimics $1/f$ distribution. Therefore, the normalizable log-normal distribution is well-approximated by a $1/f$ power-law distribution (relates to Zipf's law) over a wide but finite range in a large N limit.

2.2 $1/f$ noise from $1/f$ distribution

A purely random process has the auto-correlation of the form:

$$\begin{aligned} \langle \phi(t_1) \phi(t_2) \rangle &\sim |\phi_0|_k^2 e^{-i\omega_k(t_2-t_1)} e^{-|t_2-t_1|/\tau_c} \\ &\sim e^{-|t_2-t_1|/\tau_c}, \end{aligned} \quad (5)$$

where in the second step we ignore the real frequency part because the wave is not the concern here. We can do the Fourier transform of $e^{-|t_2-t_1|/\tau_c}$ from the time-domain to the frequency domain and obtain

$$S_{\tau_c}(\omega) \sim \frac{1/\tau_c}{1/\tau_c^2 + \omega^2} \xrightarrow{\text{large } \tau_c} \frac{1}{\omega^2}, \quad (6)$$

which τ_c introduces a time scale in the problem. Now the problem is that $1/f$ distribution is scale-free. To rescue the problem, one can consider an ensemble of random processes, each with their own correlation time τ_c . The power spectrum is then given by

$$S(\omega)_{\text{eff}} = \int_{\tau_{c1}}^{\tau_{c2}} P(\tau_c) S_{\tau_c}(\omega), \quad (7)$$

where $P(\tau_c)$ is the probability that τ_c lies in $d\tau_c$ at τ_c . It means τ_c is probabilistic-distributed as oppose to a single characteristic correlation time. Since we are motivated by scale-invariance, we can impose $P(\tau_c)$ to be scale-invariant, i.e.

$$P(\tau_c) = \frac{d\tau_c}{\tau_c}. \quad (8)$$

The power spectrum then becomes

$$S(\omega)_{\text{eff}} = \int_{\tau_{c1}}^{\tau_{c2}} \frac{d\tau_c}{\tau_c} \frac{1/\tau_c}{1/\tau_c^2 + \omega^2} = \frac{\tan^{-1} \omega\tau}{\omega} \Big|_{\tau_{c1}}^{\tau_{c2}} \sim \frac{1}{\omega}, \quad (9)$$

where the last step, $S(\omega)_{\text{eff}} \sim 1/\omega$, is valid when the scale invariance covers many decades, that is, τ_{c2}/τ_{c1} is a large ratio.

Naturally, we want a simple, intuitive model which displays $1/f$ noise and captures “Joseph” effect (sustained, persistent events) and “Noah” effect (big events) in the non-Brownian random process. The self-organized criticality will do the job.

3 Self-organized criticality

In this section, we are going to see that a spatially extended dissipative, dynamical system will naturally evolved to a self-organized critical state with no characteristic time and length scales. The *spatially extended dynamical system*, i.e. system with both spatial and temporal degrees of freedom, are everywhere in physics, biology, and economics. One class of the system is the ubiquitous temporal effect known as “ $1/f$ ” noise of which the power spectrum shows a power-law behavior $f^{-\beta}$ over a wide range of time scales. (Note: in general, $1/f$ means $1/f^\beta$ with $\beta \leq 1$.) The other class of the system is based on empirical observations that a spatially extended system tends to naturally evolve into scale-invariant, self-similar fractal structures. These two classes show that the system evolves to a critical state with power-law spatial correlation as well as $1/f$ temporal signature over several decades.

In this section, we will mostly follow this PRL paper [2] (thereafter Paper 1) and this PRA paper [3] (thereafter Paper 2), both written by Bak, Tang and Wiesenfeld (BTW). In Papers 1 & 2, BTW have numerically demonstrated that a spatially extended dissipative dynamical system naturally evolves into a self-organized critical state with both spatial and temporal power-law scaling. As we will see quickly, the spatial degrees of freedom evolves to a scale-invariant, self-similar fractal structure, and the temporal behavior is a $1/f$ noise with a power-law spectrum $S(f) \sim f^{-\beta}$.

Before we jump into the sand pile model, let's first summarize few key elements in the SOC [2, 3]:

1. Motivated by ubiquity and challenge of $1/f$ noise (scale-invariant).
2. Spatially extended excitations (also known as avalanches).
3. Collective ensemble of avalanches
4. Evolve to self-organized critical structure of states which are barely stable. Note that SOC state does not mean linearly marginal state.
5. The power-law for temporal fluctuations – the $1/f$ noise – is a combination of *dynamical* minimal stability and spatial scaling.
6. SOC is about the noise propagation through the marginally stable cluster via the “domino” effect. The noise is essential to *probe* the dynamic state.
7. The critical point is an *attractor* of the dynamics to the equilibrium state even the system may start far from equilibrium. That is, no detailed specification of the initial condition is needed.
8. Unlike the critical point at phase transitions in equilibrium statistical mechanics which can only be obtained by fine-tuning a parameter, e.g. Ginzburg-Landau theory, the SOC does not require any fine-tuning to get $1/f$ noise and fractal structure – the critical structure is *self-organized*.

3.1 One dimension sand pile and minimal stability

Let's reveal the outcome before we begin the 1D sand pile problem. Actually the 1D sand pile evolves to a least stable metastable state and has no spatial structure and uninteresting temporal behavior. It is similar to the 1D percolation problem where the only way to let the cluster to percolate is to let all sites be occupied, that is, the percolation threshold be $p_c = 1$. In terms of the sand pile models, the more interesting results happen in 2D and 3D. But for the pedagogical reason we will quickly go through the 1D sand pile model [3].

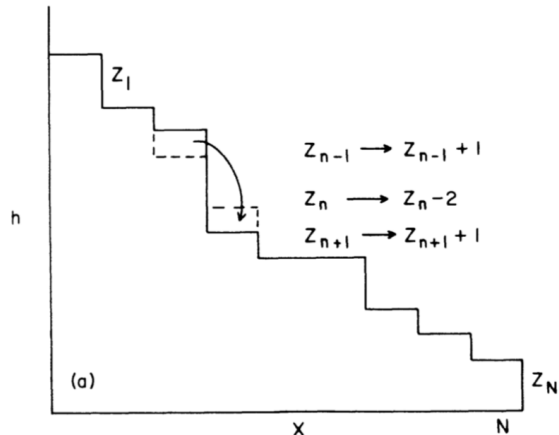


Figure 2: The figure is taken from Ref. [3]. One-dimensional sand pile of length N . The boundary condition is that the sands can leave the system at the right-hand side only. The figure shows that one unit of sand at site n tumbles to the site $n + 1$ when $z_n > z_c$.

We can build the sand by randomly adding a grain of sand at a time. Figure 2 shows the configuration of a sand pile model of length N . The right-end is a loosely boundary so that the sands can leave from the right-end. The vertical axis is the height of the sand pile; the horizontal axis is discretized to N sites. The z_n is defined as the height difference between site n and site $n + 1$, i.e. $z_n \equiv h(n) - h(n + 1)$. The machinery to add one grain of sand at the n th site is given by

$$\begin{aligned}
 z_n &\rightarrow z_n + 1, \\
 z_{n-1} &\rightarrow z_{n-1} - 1.
 \end{aligned}
 \tag{10}$$

Focus on site n for now. The sand pile will eventually grow to a critical slope where adding any more sand will lead the sand pile to slide off. We expect that there is a critical value z_c that once the difference in height is higher than z_c , one unit of sand at n th site tumbles to the lower level (to the site $n + 1$):

$$\begin{aligned}
 z_n &\rightarrow z_n - 2, \\
 z_{n\pm 1} &\rightarrow z_{n\pm 1} + 1,
 \end{aligned}
 \tag{11}$$

which is a discretized nonlinear diffusion equation. The cartoon is shown in Fig. 2. This model is a *cellular automaton* which describes the interaction of the state variable z_n at time $t + 1$ with its neighbors at time t .

If we add more and more sands randomly in space, the sand pile will eventually reach a critical state z_c that any addition of sand grains will just fall from site to site, eventually reaching the site N and exiting the system. The system then reaches the *minimally stable state*. (The maximally stable state is, of course, an empty 1D sand pile system.) When the 1D sand pile system reaches the critical state, the falling grains (sandflow) as a transport will

flow through the system, but the system is immune to the noise and eventually reaches the globally minimally stable state again. This sandflow is a random white noise with the power spectrum scaled as $1/f^0$. As a result, the 1D sand pile problem has no interesting temporal signature and there is no spatial structure.

However, in the following subsection, we will show that in 2D and 3D sand pile systems the minimally stable state is unstable with respect to small fluctuations and the spatial and temporal structures stem from scale-invariant, self-similar fractal structures.

3.2 SOC in two and three dimensions

In two-dimension, the rules for adding one grain and the grain-tumbling in cellular automation are given by [3]

$$\begin{aligned} z(x-1, y) &\rightarrow z(x-1, y) - 1, \\ z(x, y-1) &\rightarrow z(x, y-1) - 1, \\ z(x, y) &\rightarrow z(x, y) + 2, \end{aligned} \tag{12}$$

and

$$\begin{aligned} z(x, y) &\rightarrow z(x, y) - 4, \\ z(x \pm 1, y) &\rightarrow z(x \pm 1, y) + 1, \\ z(x, y \pm 1) &\rightarrow z(x, y \pm 1) + 1, \text{ for } z > z_c, \end{aligned} \tag{13}$$

respectively. We have assumed that the system is a 2D array (x, y) with $1 \leq x, y \leq N$, and the fixed boundary condition is used, i.e. $z = 0$ at the boundaries. Figure 3 demonstrates the sand tumbling in Eq. 13 – four grains of sands at site (x, y) tumbles to 4 adjacent neighbors.

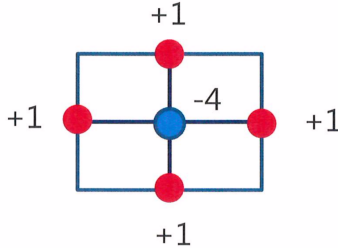


Figure 3: The tumbling of four grains at the site (x, y) .

As we have shown in the last subsection, the 1D sand pile system will eventually evolve to a minimally stable state where the slope reaches a critical value. Any newly added grain of sand will just tumble from one site to the next site and to the next, eventually reach to the boundary and exit the system. The critical state is *stable* with respect to small fluctuations. However, the 2D and 3D sand pile systems have very different behavior. Assuming a 2D sand pile at a minimally stable state, when the site (x, y) topples, four grains of sand tumbles to four adjacent points. Immediately, the four adjacent points become unstable with respect

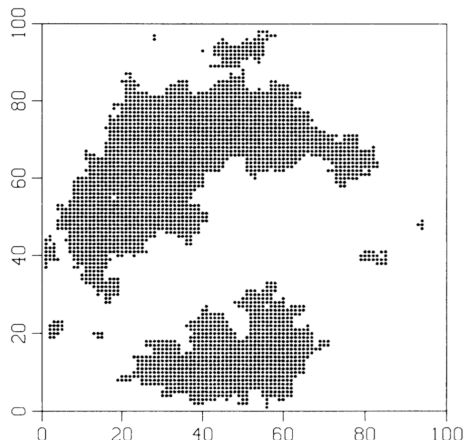


Figure 4: Figure is taken from Ref. [2]. The domain structure of local perturbations. The grid size is a 100×100 array.

to this toppling and they each tumbles 4 grains of sand to the adjacent neighbors. The noise spread out to the neighbors, then their neighbors, and eventually the noise propagate throughout the entire system. Comparing to 1D sand pile problem, we find that the 2D sand pile does not have a stable minimally stable state with respect to small fluctuations and thus the minimally stable state is not an attractor of the dynamics to the equilibrium. Instead of getting minimally stable states in 2D problem, we expect to get a lot of more-than-minimally stable states and these states will prevent the propagation of noise.

When will the system become stable? As observed by BTW in Paper 1 and 2, the stability will be reached precisely at the point when all the minimally stable states cascade to an ensemble of more-than-minimally stable states at the level where the noise can no longer spread out to infinity. This dynamical system naturally evolve to a self-organized critical state with no characteristic length and time scales.

Figure 4 shows the domain structure resulted from several single-site-induced perturbations. The dark areas represent the clusters affected by the toppling of a single site interior.

Figure 5a shows the distribution of cluster size of a 2D sand pile system, averaged over 200 samples. The distribution of cluster size sticks to a power-law for at least two decades,

$$D(s) \approx s^{-\tau}, \tau \approx 1.0 \quad \text{for 2-dimension,} \quad (14)$$

which suggests the system is actually at a critical state with spatial scaling of the clusters. The deviation at small size comes from the discreteness effect of the lattice. The deviation from the power-law at large cluster size is a finite-size effect.

Figure 5b shows the distribution of lifetime weighted by the average response s/t . The numerical simulation result also shows a temporal power-law scaling:

$$D(t) \approx t^{-\alpha}, \alpha \approx 0.43 \quad \text{for 2-dimension.} \quad (15)$$

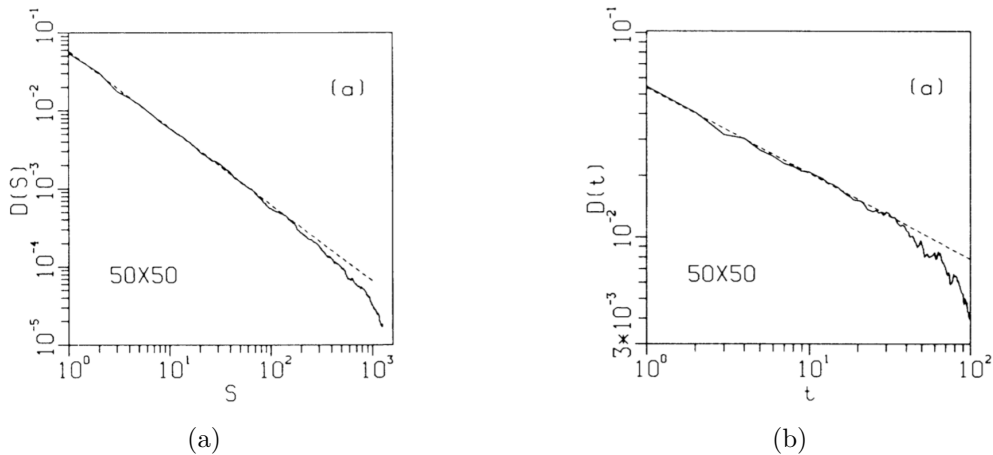


Figure 5: Figures are taken from Ref. [2]. (a) Distribution of cluster size at the critical state. The grid size is 50×50 , averaged over 200 samples. (b) Distribution of lifetimes of the clusters corresponding to (a).

We can interpret the sliding as energy dissipation. The cluster of size s represents the total energy dissipation due to a single avalanche. If each sliding has its own correlation time T , the autocorrelation has the form $\sim e^{-t/T}$ and the Fourier transformation representation is $\sim T / (1 + (\omega T)^2)$. The power spectrum is then given by

$$S(\omega) = \int \frac{T}{1 + (\omega T)^2} D(T) dT \sim \omega^{-2+\alpha} = \omega^{-\beta}. \quad (16)$$

The 2D sand pile has $\alpha = 0.43$ and $\beta = 1.57$ for a 50×50 grid. The 3D sand pile has $\alpha \approx 0.92$ and $\beta \approx 1.08$ for a $20 \times 20 \times 20$ grid. Both models indicate a temporal power-law scaling – the $1/f$ noise.

The numerical simulation clearly indicates that the dynamical, dissipative system evolves to a self-organized critical state with a scale-invariant fractal structure and the $1/f$ noise. Physically this result means the dynamical system self-organizes itself to minimally stable states on all length scales with power-law spatial scaling, and the energy dissipation of each cluster avalanche is turned into temporal power-law fluctuations on all time scales.

3.3 Analogies between the sandpile transport and turbulent transport

The sandpile problem, or the Kadanoff model [6], only receives interesting dynamics if the system size is much larger than the interspacing between two consecutive sites, i.e. $L/\Delta \sim N \gg 1$. This is precisely analogous to $\rho_* \ll 1$ condition in turbulent transport. The Kadanoff model naturally motivates an analogy with magnetic fusion energy (MFE). We will compare sand pile with confinement.

Analogies between sandpile transport & turbulent transport	
Sand pile	MFE confinement
Grid site	Local fluctuations
Toppling rules	Local turbulence mechanism
Δz_{crit}	“Critical gradient” for local instability
Number of unstable grains N	Local eddy-induced transport
Random rain of grains	External heating
Sand flux	Heat/particle flux
Average slope	Mean profile
Avalanche	Transport event
Fractal profile	Choppy profile
Sheared wind	Sheared electric field
Local rigidity	Profile stiffness

3.4 Definition of SOC

Now let’s give SOC a more precise definition. The reader is encouraged to read Jenson’s book [7]. There are two types of definition:

- The constructive definition: a slowly driven, interaction dominated threshold system. The classic example is sand pile.
- The phenomenological definition: the system exhibit a power-law scaling without tuning. The special note is $1/f$ noise, also known as flicker shot noise.

The elements in SOC are:

1. Slowly driven, interaction-dominated threshold system, e.g. sand pile.
2. Many degree of freedom
3. The dynamics are dominated by degree of freedom couplings, i.e. cell-cell interaction dominated.
4. Need threshold and slow drive. (“Strong” v.s “slow” is set by toppling rules.)
5. Local criterion for excitation (otherwise you will lose spatial separation).
6. Large number of accessible meta-stable sates.
7. Local profile rigidity, which is analogous to “profile stiffness” in MFE confinement.

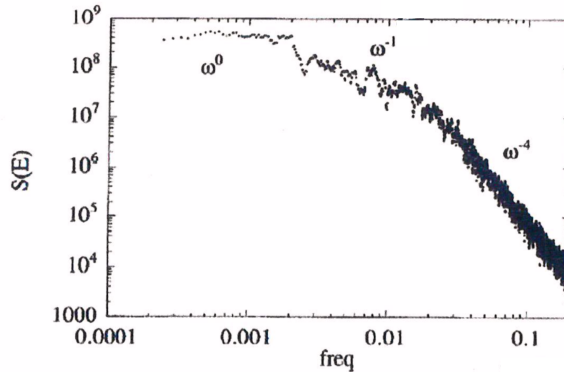


Figure 6: Generic power spectrum of over-turnings $\langle(\Delta Z)^2\rangle_\omega$ v.s frequency.

3.5 Generic spectra of SOC

There is a generic spectra that emerges from the SOC. As shown in Fig. 6, the ω^{-1} manifests in middle range of the frequency. At higher frequency, we get ω^{-4} or some much higher power of ω , and at the lower frequency range we have ω^0 . The ω^{-1} range is hand-in-hand with $H \rightarrow 1$, which suggests avalanche. In the language of Mandelbrot [1], they suggest “Joseph” – that avalanche is a persistent event. The ω^0 range corresponds to large events and the lower frequency events get most power. In the Mandelbrot terminology, they are “Noah”. The ω^{-4} range corresponds to uncorrelated overturning (localized events) so the self-correlation dominates the dynamics.

4 Continuum hydrodynamic models

There are similarities between SOC and cascades in fluid turbulence. One may ask: is there a hydrodynamical model for the SOC? Can we describe the system on scale l which is less than system size, L , but much greater than grain size, Δ ? We want to develop a hydrodynamical model of the mean field criticality. The classic paradigm is Ginzburg-Landau theory, which the key idea is *symmetry*. Take the magnetization for example:

$$\frac{dn}{dt} - c\nabla^2 n = -a(T - T_c)n - bn^3. \quad (17)$$

When $T < T_c$, the ground state changes, and this is known as external tuning. The critical feature is the use of symmetry. Also there is an implicit universality that any thing that has the right symmetry and the right general structure can be written in the form of Ginzburg-Landau theory. Note that the classic Ginzburg-Landau theory is *externally tuned*, i.e. it has an externally tuned criticality.

The idea above brings us to the hydrodynamical theory of SOC. We are interested in a continuum model which is reminiscent to Burger turbulence. The criteria for SOC continuum

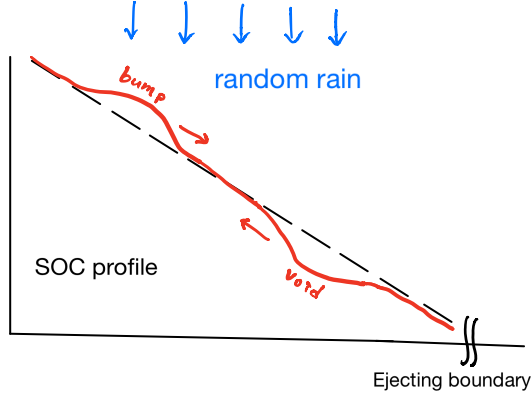


Figure 7: An 1D box with ejecting boundary on the right-hand side. The dashed line is the SOC profile. The red curve is the deviation from SOC.

hydro model is $L \gg l \gg \Delta$. In terms of time scale, the time has to be much longer than the time for a step but much shorter than the confinement time, i.e. $\tau_{\text{confinement}} \gg \tau \gg \tau_{\text{step}}$.

Consider a 1D box with ejecting boundary on the right-hand side and accumulating boundary on left-hand side. See Fig. 7. Imagine there is a SOC profile, the dashed line, and the random grains fall in. The deviation from SOC profile is made by bumps, “blobs”, and the voids, “holes”, and is shown as the red curve.

Assuming the conservation of “stuff” in the profile up to the boundary losses, we write the density of “stuff” as P , which can be interpreted as the pile or system occupation. The idea is then to write the dynamics of deviation from SOC state as

$$P \equiv P_{\text{soc}} + \delta P. \quad (18)$$

We are interested in the evolution of δP . The governing equation for δP is the conservation of P ,

$$\partial_t \delta P + \partial_x \left[\Gamma(\delta P) - D_0 \partial_x \delta P \right] = \tilde{S}, \quad (19)$$

where $\Gamma(\delta P)$ is the flux induced by deviation from SOC profile. (Note that Eq. 19 can be extended to higher order dimension, see Ref. [8].) Obviously, P is conserved up to the boundary, so δP evolution is governed by $\nabla \cdot \Gamma$ term. To constrain $\Gamma(\delta P)$, we shall seek *symmetry*, in the spirit of Ginzburg-Landau prescription.

Suppose we have a flat system, and now we make a bump. The bump will spread out but still conserve the area. Likewise, the void will be filled by two sides. For the case of a bump on a slope, the downslope extends, and the bump goes down and to the left. Likewise, the void on the slope has greater extend on upslope, and the void will go up and to the left. See the red arrows in Fig. 7.

In the mind of symmetry, we observe the joint reflection, $x \rightarrow -x$. The other symmetry is the flip of bumps and voids, which is described as $\delta P \rightarrow -\delta P$. The bump is going down

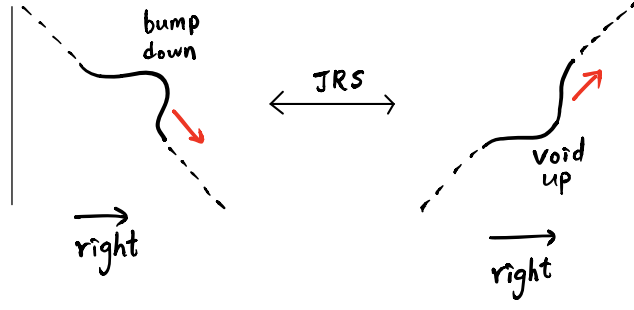


Figure 8: Bump-void interaction.

and to the right, and the void is going up and to the right. So either way, they go to the right – they have the same flux direction. See Fig. 8 for cartoon explanation. This observation brings us to the principle of Joint Reflection Symmetry (JRS), i.e.

$$\Gamma(\delta P) \Big|_{\substack{x \rightarrow -x \\ \delta P \rightarrow -\delta P}} = \Gamma(\delta P), \quad (20)$$

which actually puts quite a big constraint on the form of $\Gamma(\delta P)$.

We are interested in seeking the flux in the large scale ($l \gg \Delta_{\text{grain}}$) and long time ($\tau \gg \tau_{\text{step}}$). However, the structure of full flux is, in principle, very complicated. To make progress, we can once again learn from our beloved Ginzburg-Landau theory – write down the general form of the free-energy and eliminate terms that don't satisfy the symmetry criteria. In the case of SOC, the general form of flux is given by

$$\Gamma(\delta P) = \sum_{m,n,q,r,\alpha} \left\{ \underbrace{A_n (\delta P)^n}_1 + \underbrace{B_m (\partial_x \delta P)^m}_2 + \underbrace{D_\alpha (\partial_x^2 \delta P)^\alpha}_3 + \underbrace{C_{q,r} (\delta P)^q (\partial_x \delta P)^r}_4 + \dots \right\}. \quad (21)$$

There are four terms in Eq. 21. Let's apply JRS, $x \rightarrow -x$ and $\delta P \rightarrow -\delta P$, to all of them.

1. $n = 1$ violates JRS because $\delta P \rightarrow -\delta P$; on the other hand, $n = 2$ preserves it.
2. $m = 1$ is ok because the product of x and δP is invariant under JRS, so as $m = 2$.
3. $\alpha = 1$ violates JRS. While $\alpha = 2$ is ok, there are two dependence on the fine scales so we don't consider it.
4. $q = 1$ and $r = 1$ violates JRS. If we go to higher power, the dependence on δP would be too high, so we ignore them.

To the lowest order, we have

$$\partial_t \delta P + \partial_x \left[A_2 (\delta P)^2 + B_1 \partial_x \delta P + B_2 (\partial_x \delta P)^2 + D_2 (\partial_x^2 \delta P)^2 - D_0 \partial_x \delta P \right] = \tilde{S}. \quad (22)$$

We can combine B_1 and D_0 since they have the same form. For $(\partial_x \delta P)^2$ and $(\partial_x^2 \delta P)^2$, they are fine at the lowest order, but since they have an extra order of derivative, meaning they are probing the smaller scale, we ignore them. After some simplification, we obtain

$$\partial_t \delta P + \partial_x \left[\alpha (\delta P)^2 - D \partial_x \delta P \right] = \tilde{S}, \quad (23)$$

which is widely known as Noisy Burger’s Equation¹. The noisy Burger’s equation also supports the discontinuity solution that has shock properties.

The classical Burger’s equation is the one-dimensional Navier-Stoke equation for a pressure-less fluid,

$$\partial_t v + v \partial_x - \nu \partial_x^2 v = \tilde{S}. \quad (24)$$

For $\tilde{S} = 0$, the exact solvable Burger’s equation is shock. Note that the speed of the shock is proportional to the amplitude. Big guys go faster and eat smaller guys.

References

- [1] Benoit B. Mandelbrot and James R. Wallis. Noah, joseph, and operational hydrology. *Water resources research*, 4(5):909–918, 1968.
- [2] Per Bak, Chao Tang, and Kurt Wiesenfeld. Self-organized criticality: An Explanation of 1/f noise. *Phys. Rev. Lett.*, 59:381–384, 1987.
- [3] Per Bak, Chao Tang, and Kurt Wiesenfeld. Self-organized criticality. *Phys. Rev.*, A38:364–374, 1988.
- [4] Aldert Van Der Ziel. On the noise spectra of semi-conductor noise and of flicker effect. *Physica*, 16(4):359–372, 1950.
- [5] Elliott W. Montroll and Michael F. Shlesinger. On 1/f noise and other distributions with long tails. *Proceedings of the National Academy of Sciences*, 79(10):3380–3383, 1982.
- [6] Leo P. Kadanoff, Sidney R. Nagel, Lei Wu, and Su-min Zhou. Scaling and universality in avalanches. *Physical Review A*, 39(12):6524, 1989.
- [7] Henrik Jeldtoft Jensen. *Self-organized criticality: emergent complex behavior in physical and biological systems*, volume 10. Cambridge university press, 1998.
- [8] Terence Hwa and Mehran Kardar. Avalanches, hydrodynamics, and discharge events in models of sandpiles. *Physical Review A*, 45(10):7002, 1992.

¹“If you work in classical theoretical physics, sooner or later you will be flipping burgers” – P. H. Diamond